SLAC-108
UC-37
December 1969
(EXPI)

PULSE SHAPE IN MULTIWIRE PROPORTIONAL WIRE CHAMBER

SANJIT K. MITRA*
STANFORD LINEAR ACCELERATOR CENTER
STANFORD UNIVERSITY
Stanford, California

PREPARED FOR THE U.S. ATOMIC ENERGY
COMMISSION UNDER CONTRACT NO. AT(04-3)-515

December 1969

*Visiting Scientist from University of California, Davis, California.

TABLE OF CONTENTS

There has been recently an increasing interest in the use of multiwire proportional counters as profile monitors for weak secondary beams.[1-3] It is thus of interest to determine analytically the pulse shape that would be obtained in such a chamber.

The details of construction of a multiwire chamber are described elsewhere. The cross section of a chamber[1] drawn perpendicular to the beam is shown in Fig. 1. The outer electrodes consists of two rectangular planes of stainless-steel meshes at the center of which are stretched very thin stainless-steel wires. In a typical chamber the distance between the outer electrodes is 14 mm, wire separation is 2 mm and the diameter of the wires is 50 μ. Each central wire is connected to an individual preamplifier. The circuit block diagram will be found in Ref. 3. When used for monitoring, a suitable gas such as argon-CO_2 mixture (90 - 10) is circulated between the electrodes.

It has been shown by Charpak *et al.*[1] that the equipotentials near the wires are concentric to the wires. Due to the high field intensity confined to the region near the wires, most of the gas multiplication occurs within a few mean free paths of the wires. Thus, we expect the properties of the multiwire chamber to be similar to that of the single wire co-axial cylindrical proportional counter. This has also been verified experimentally by Charpak *et al.*[1]

A. Principle of Operation

To determine the pulse shape in a cylindrical co-axial counter, we follow the analysis technique outlined by Wilkinson.[4,5] A simplified schematic diagram of such a chamber along with the amplifier input circuit is shown in Fig. 2, where C is the sum of chamber capacity and the input strays, and R is the input impedance of the preamplifier. Note that with no ionization, $v_a(t) = 0$. When a weak particle passes through the chamber, N_p primary ion pairs are formed by initial ionization. The positive ions are attracted by the outer electrodes and the primary electrons are attracted toward the central wire. In the vicinity of the wire these electrons gain sufficient energy to produce secondary ion pairs by collision with neutral gas molecules. If M represents the gas multiplication factor of the chamber, then this corresponds to MN_p ion pairs with charge $+ MN_pe$ and $- MN_pe$ where e is the electronic charge. The negative charge will

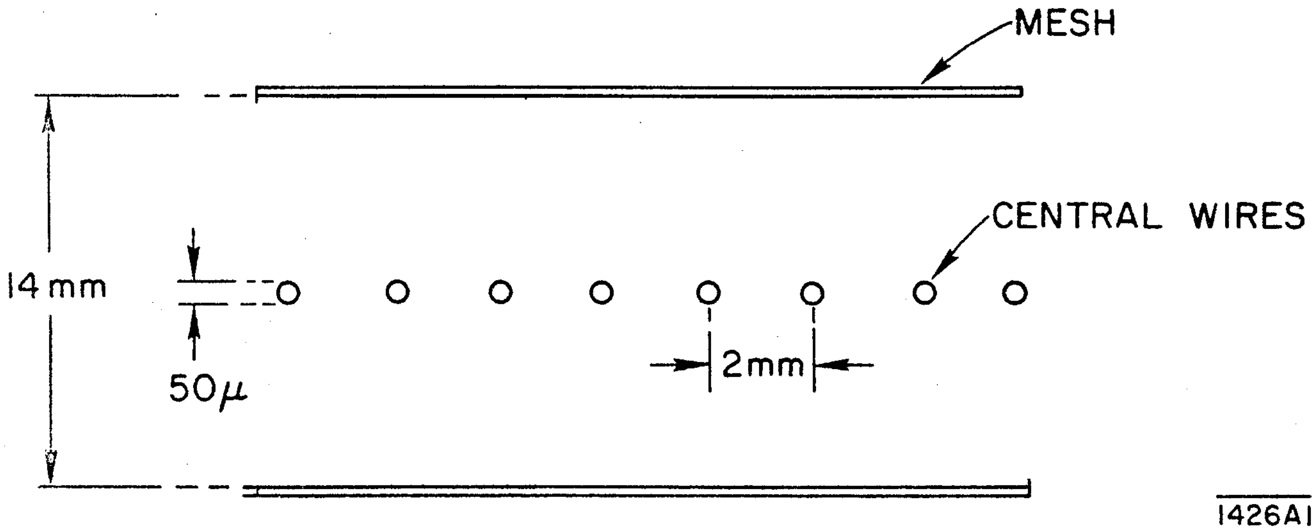

Fig. 1

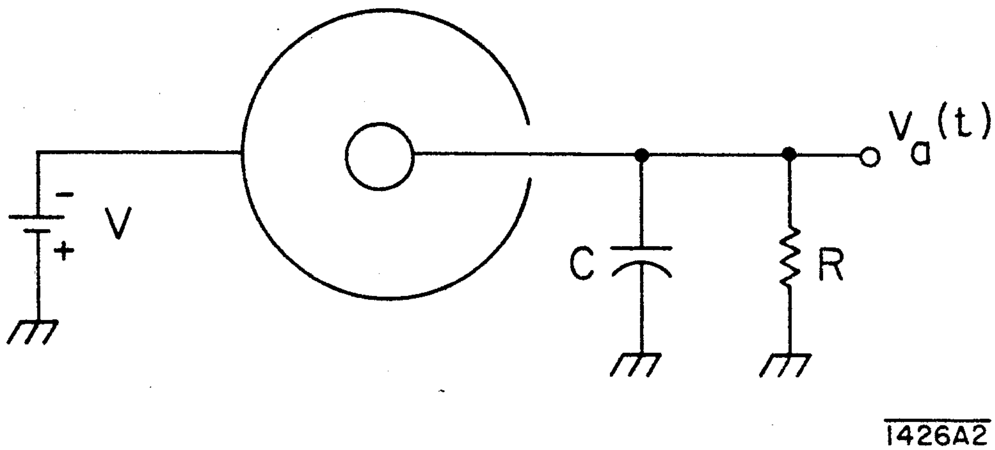

Fig. 2

be attracted to the central wire (anode) and the positive charge to the high voltage electrode. Thus there will be a change in the charge stored on the electrodes due to the collection of these ions and consequently $v_a(t)$ will change from zero to some finite value. The secondary electrons (which have very high mobility) being formed very near the anode (within a distance of the order of the radius of the wire) will be collected almost immediately. As a result, the voltage pulse $v_a(t)$ appearing at the anode is produced almost exclusively from induction by the positive ions as they move away from the anode. Since the positive ions move through most of the voltage drop in the high field region near the anode, the voltage pulse produced by the positive ion movement will have a very fast rise time.

B. Pulse Shape Evaluation — Amplifier with Infinite Bandwidth

Consider now the case for which RC is much greater than the time t_+ required to collect all the positive ions. This in effect implies that there is no leakage through R or in other words, the effect of R can be neglected. (Later in this report we consider the effect of R on the pulse shape.) Under this condition, we then have

$$v_a(t) = \frac{q(t)}{C} \tag{1}$$

where q(t) is the net charge produced by the positive ions and electrons. If $-q_+(t)$ and $-q_-(t)$ are the charges induced on the electrodes by the positive and negative charges, equal charges of opposite sign appear across the capacitor C and we can write

$$v_a(t) = \frac{q_+(t) + q_-(t)}{C} \tag{2}$$

To evaluate the induced charges we invoke Green's theorem.[6] According to this theorem, if a set of conductors 1, 2, and 3 have potentials V_1, V_2, and V_3 due to placing of charges q_1, q_2, and q_3 on them, then by placing charges q_1', q_2', and q_3' on them will result in potentials V_1', V_2', and V_3' where

$$q_1V_1' + q_2V_2' + q_3V_3' = q_1'V_1 + q_2'V_2 + q_3'V_3 \tag{3}$$

Consider now the co-axial chamber redrawn in Fig. 3. Let q_a be the charge induced on the anode and q_b be the charge induced on the outer cylinder due to a

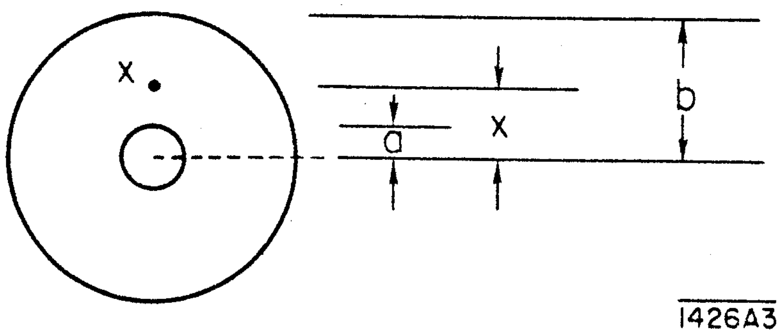

Fig. 3

charge q located at a point x between them. Since the outer electrode completely encloses the anode, all the lines of force from q end on either the anode or the outer electrode, and hence

$$q + q_a + q_b = 0 \tag{4}$$

In the absence of a charge at x (i.e., q' = 0), let V'_a, V'_b, and V'_x be the respective potentials. Just prior to ion pair formation, $V_a = V_b = 0$ which is also the case soon after the charge q is produced. Equation (3) thus reduces to

$$q_a V'_a + q_b V'_b + q V'_x = 0 \tag{5}$$

Solving Eqs. (4) and (5) one obtains

$$q_a = \frac{V'_b - V'_x}{V'_a - V'_b}\, q \tag{6}$$

In a co-axial cylinder, the potential differences are given by[7]:

$$V'_a - V'_b = -\int_b^a \frac{q'_a\, dr}{2\pi \epsilon r} = \frac{q'_a}{2\pi\epsilon} \ln\left(\frac{b}{a}\right) \tag{7}$$

$$V'_x - V'_b = -\int_b^x \frac{q'_a\, dr}{2\pi \epsilon r} = \frac{q'_a}{2\pi\epsilon} \ln\left(\frac{b}{x}\right) \tag{8}$$

Thus

$$\frac{V'_x - V'_b}{V'_a - V'_b} = \frac{\ln(b/x)}{\ln(b/a)} \tag{9}$$

From Eqs. (6) and (9) we thus obtain

$$q_a = -\frac{\ln(b/x)}{\ln(b/a)}\, q \tag{10}$$

If we denote by r_+ and r_- the positions of the positive ion and the free electron respectively, then from Eq. (10) the charge induced on the anode by a positive ion at r_+ and a free electron at r_- are given as:

$$q_+(t) = -\frac{\ln(b/r_+)}{\ln(b/a)}\, e \tag{11}$$

and

$$q_-(t) = \frac{\ln(b/r_-)}{\ln(b/a)}\, e \tag{12}$$

Use of Eqs. (11) and (12) in Eq. (2) results in

$$\begin{aligned} v_a(t) &= -\frac{MN_p e}{C}\left[\frac{\ln(b/r_+)}{\ln(b/a)} - \frac{\ln(b/r_-)}{\ln(b/a)}\right] \\ &= -\frac{MN_p e}{C}\left[\frac{\ln(r_-/r_+)}{\ln(b/a)}\right] . \end{aligned} \tag{13}$$

Assuming that the ion pairs are formed at the anode and the current is carried entirely by the motion of positive ions so that motion of electrons can be neglected, Eq. (13) becomes

$$v_a(t) = -\frac{MN_p e}{C} \cdot \frac{\ln(a/r_+)}{\ln(b/a)} \tag{14}$$

where we have used $r_- = a$. Note from (14) that when the positive ions reach the outer electrode $r_+ = b$, and the pulse height reaches its maximum value v_{max}:

$$v_{max} = \frac{MN_p e}{C} \tag{15}$$

Even though in general the motion of positive ions is random, there is a net drift in the direction of the electric field. The average drift velocity dr_+/dt is given as:

$$\frac{dr_+}{dt} = \mu\, \frac{\mathscr{E}}{p} . \tag{16}$$

where μ is the mobility of the ion, $\mathscr{E}$ is the electric field strength at r_+ and p is the gas pressure. In a co-axial chamber the electric field strength, $\mathscr{E}$, at a distance r_+ from the center can be computed from[7]

$$\mathscr{E} = \frac{V}{r_+ \ln(b/a)} \tag{17}$$

where V is the potential difference between the two electrodes. Combining Eqs. (16) and (17) we thus have

$$\frac{dr_+}{dt} = \frac{\mu V}{pr_+ \ln(b/a)} \tag{18}$$

Equation (18) can be solved as follows. We rewrite it as:

$$r_+ dr_+ = \frac{\mu V}{p \ln(b/a)} \cdot dt$$

Therefore

$$\int r_+ \, dr_+ = \frac{\mu V}{p \ln(b/a)} \int dt + k$$

or

$$\frac{r_+^2}{2} = \frac{\mu V t}{p \ln(b/a)} + k \tag{19}$$

Assuming that all positive ions start at $r_+ = a$ at $t = 0$, we get $k = a^2/2$. Therefore

$$r_+ = \left[\frac{2V\mu t}{p \ln(b/a)} + a^2 \right]^{1/2} \tag{20}$$

Substituting expression (20) in Eq. (14), we get the desired expression for the voltage across the capacitor:

$$\begin{aligned} v_a(t) &= \frac{MN_p e}{C \ln(b/a)} \ln \left\{ \frac{1}{a} \left[\frac{2V\mu t}{p \ln(b/a)} + a^2 \right]^{1/2} \right\} \\ &= \frac{MN_p e}{2C \ln(b/a)} \ln \left\{ \frac{2V\mu t}{a^2 p \ln(b/a)} + 1 \right\} \end{aligned} \tag{21}$$

The total time t_+ required to complete collection of the positive ions can be found from Eq. (20) by letting $r_+ = b$:

$$t_+ = \frac{p \ln(b/a)}{2V\mu} (b^2 - a^2) \tag{22}$$

For the typical wire chamber shown in Fig. 1, we can consider each wire to form a co-axial proportional chamber with the outer electrode having

$$b = 7 \text{ mm} = 0.7 \text{ cm}$$
$$a = 1 \text{ mil} = 2.54 \times 10^{-3} \text{ cm} \tag{23}$$

For a 4000 V voltage across the two electrodes containing argon as the filling gas at 1 atm pressure, we obtain from Eq. (22):

$$t_+ = \frac{\left[(0.7)^2 - (2.54\times 10^{-3})^2\right] 760}{2(4000)\ (1.04 \times 10^3)} \ \ell n \left(\frac{700}{2.54}\right)$$
$$\cong 262\ \mu\text{sec} . \tag{24}$$

Note that the value of μ used to derive the above is 1040 (cm/sec) $(\text{volt/cm})^{-1}$ (mm Hg).[8]

The normalized response for this typical chamber is shown in Fig. 4.

For brevity, let us normalize the time and the magnitude and rewrite Eq. (21) as:

$$v_n(\tau) = \frac{\ell n \left\{ \frac{b^2}{a^2} \tau + 1 \right\}}{2\ \ell n(b/a)} \tag{25}$$

where now

$$\tau = \frac{2V\mu}{b^2 p\ \ell n(b/a)} \cdot t \tag{26}$$

Note that the time τ_+ taken by the positive ions to reach the outer electrode is

$$\tau_+ = 1 - \frac{a^2}{b^2} \tag{27}$$

Let us now consider the effect of R on the pulse shape. We shall show that for RC values comparable to τ_+, the effect is to obtain a pulse of shorter duration by differentiating the original pulse $v_n(\tau)$. To determine the pulse shape at the input of the amplifier, the circuit reduces to that shown in Fig. 5, where we have replaced the charged capacitor C having a initial voltage $v_n(\tau)$ across it by a series combination of a uncharged capacitor C and a voltage source $v_n(\tau)$ where

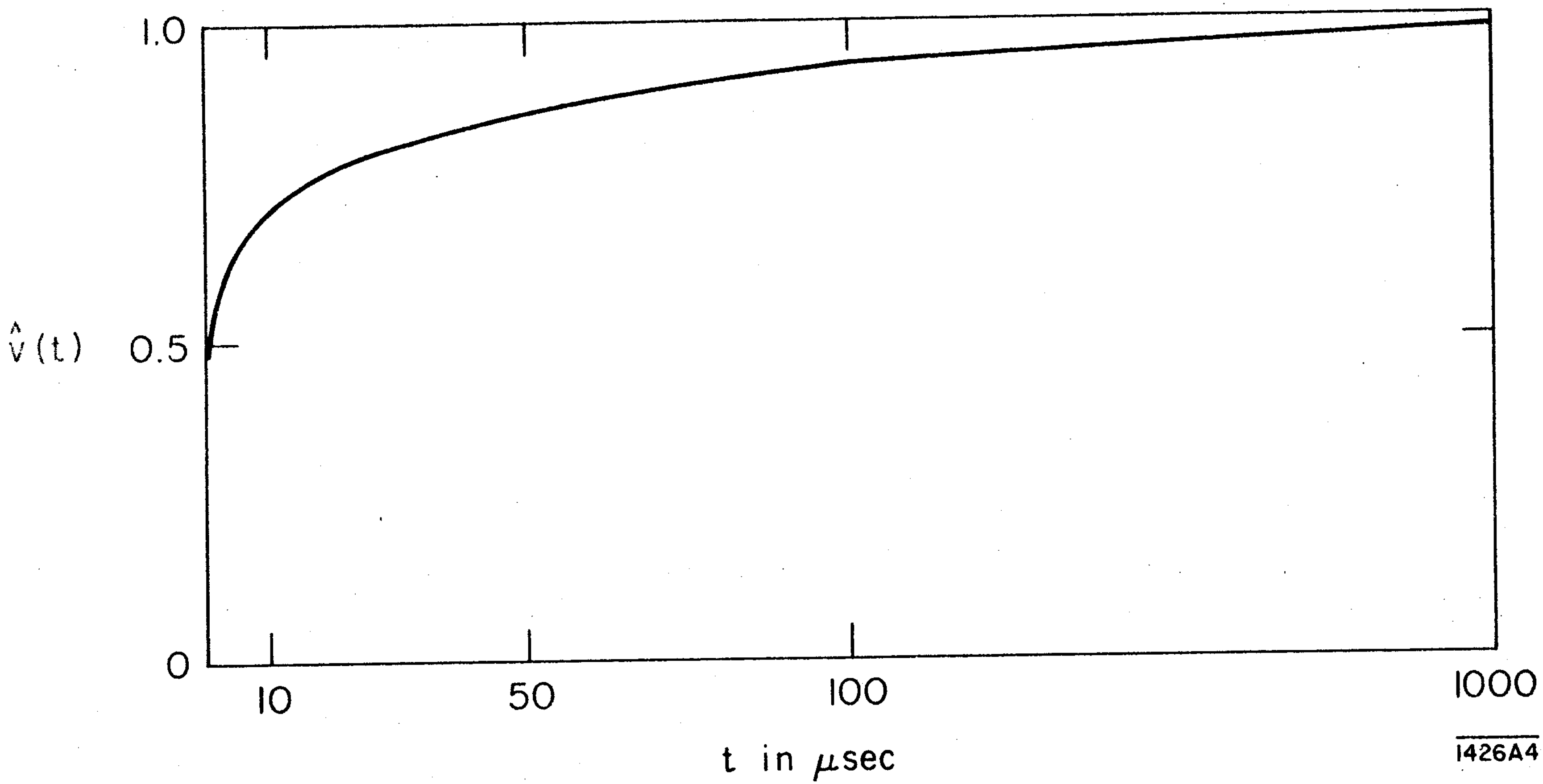

Fig. 4

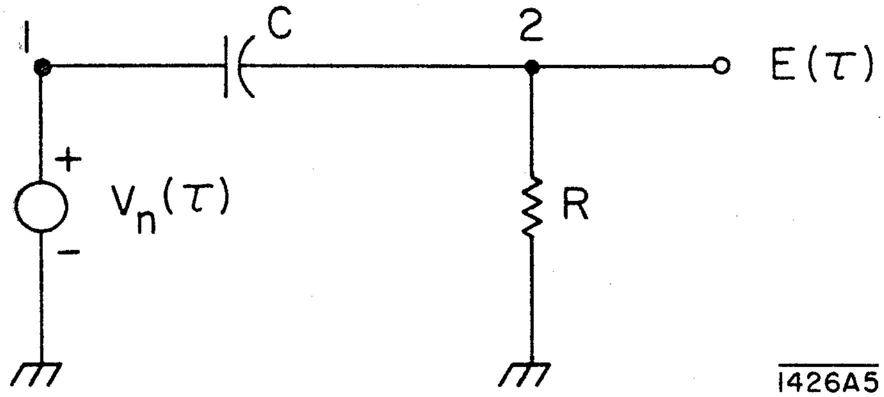

Fig. 5

$v_n(\tau)$ is given by Eq. (25). The voltage at the input of the amplifier is then given by $E(\tau)$ which in effect will be the shape of the pulse at the output of the amplifier if the amplifier has an infinite bandwidth. Summing the current at node 2 of Fig. 5, we obtain

$$C \frac{d}{d\tau} \left[v_n(\tau) - E(\tau) \right] - \frac{E(\tau)}{R} = 0 \tag{28}$$

In a typical case $R = 400\Omega$ and $C = 20$ pf. Thus $RC = 8 \times 10^{-9} \ll 1$. Under this condition, Eq. (28) reduces to

$$E(\tau) \cong RC \frac{dv_n(\tau)}{d\tau} \tag{29}$$

which indicates the differentiating property of the circuit.

The differential equation given by (28) can be written as

$$\frac{dE}{d\tau} + \gamma E(\tau) = Q \tag{30}$$

where

$$\gamma = \frac{1}{RC}$$

$$Q = \frac{dv_n}{d\tau} = \frac{1}{2\, \ln(b/a) \cdot \left(\tau + \frac{a^2}{b^2}\right)} \tag{31}$$

Solution of Eq. (30) is given as

$$E(\tau) = e^{-\int_{-\infty}^{\tau} \gamma dx} \cdot \int_{-\infty}^{\tau} Q \cdot e^{\int_{-\infty}^{x} \gamma dy} \cdot dx + k\, e^{-\int_{-\infty}^{\tau} \gamma dx}$$

$$= e^{-\gamma\tau} \int_{-\infty}^{\tau} \frac{e^{\gamma x}}{2\, \ln(b/a) \left(x + \frac{a^2}{b^2}\right)} dx + k\, e^{-\gamma\tau}$$

$$= \frac{e^{-\gamma\left(\tau + \frac{a^2}{b^2}\right)}}{2\,\ell n(b/a)} \int_{-\infty}^{\tau + \frac{a^2}{b^2}} \frac{e^{\gamma y}}{y}\, dy + k\, e^{-\gamma\tau}$$

$$= \frac{e^{-\gamma\left(\tau + \frac{a^2}{b^2}\right)}}{2\,\ell n(b/a)} \int_{-\infty}^{\gamma\left(\tau + \frac{a^2}{b^2}\right)} \frac{e^{z}}{z}\, dz + k\, e^{-\gamma\tau}$$

$$= \frac{e^{-\gamma\left(\tau + \frac{a^2}{b^2}\right)}}{2\,\ell n(b/a)} \bar{E}i \left\{\gamma\left(\tau + \frac{a^2}{b^2}\right)\right\} + k\, e^{-\gamma\tau} \qquad (32)$$

In expression (32), we have used the notation

$$\bar{E}i(x) = \int_{-\infty}^{x} \frac{e^{y}}{y}\, dy \qquad (33)$$

$\bar{E}i(x)$ is known as the exponential integral and its value for various values of x are tabulated in Ref. 9. The constant k is determined from the condition $E(0) = 0$. Thus

$$k = -\frac{e^{-\gamma a^2/b^2}}{2\,\ell n(b/a)} \cdot \bar{E}i \left\{\gamma \frac{a^2}{b^2}\right\} \qquad (34)$$

Substituting (34) in (32) we obtain the desired expression:

$$E(\tau) = \frac{e^{-\gamma\left(\tau + \frac{a^2}{b^2}\right)}}{2\,\ell n(b/a)} \left[\bar{E}i \left\{\left(\tau + \frac{a^2}{b^2}\right) \gamma\right\} - \bar{E}i\left(\frac{a^2}{b^2}\gamma\right)\right] \qquad (35)$$

= voltage out with finite R.

C. Effect of Finite Bandwidth of Amplifier[10]

An amplifier of finite bandwidth can be represented by a transfer function of the form $1/T_2\left[s + (1/T_2)\right]$ to a first order of approximation. Thus, the equivalent circuit of the proportional chamber including the input differentiating circuit will be of the form shown in Fig. 6, where $\hat{v}_a(t)$ represents the normalized voltage produced across the capacitor C if R was infinite and if the amplifier bandwidth was infinite. The expression for $\hat{v}_a(t)$ has been calculated earlier and is given as:

$$\hat{v}_a(t) = + \frac{1}{2\,\ell n(b/a)}\,\ell n\left\{\frac{2V\mu t}{2p\,\ell n(b/a)} + 1\right\} \tag{36}$$

$\hat{v}_a(t)$ is plotted in Fig. 4 for a typical case. For determining the approximate shape of $v_b(t)$ it is convenient to represent $\hat{v}_a(t)$ as shown in Fig. 7. Thus we can approximate $\hat{v}_a(t)$ as:

$$\hat{v}_a(t) \cong \frac{1}{T}\left\{t\,u(t) - (t - T)\,u(t - T)\right\} \tag{37}$$

where u(t) is the unit step function. Analysis of the equivalent circuit yields:

$$V_b(s) = \left(\frac{R}{R + \frac{1}{sC}}\right)\left(\frac{1/T_2}{s + \frac{1}{T_2}}\right)\hat{V}_a(s) = \frac{\left(1/T_2\right)s}{\left(s + \frac{1}{T_1}\right)\left(s + \frac{1}{T_2}\right)}\hat{V}_a(s) \tag{38}$$

where $V_a(s) = \mathscr{L}\left\{v_a(t)\right\}$ and $V_b(s) = \mathscr{L}\left\{v_b(t)\right\}$, $T_1 = R\,C$.

Now

$$\hat{V}_a(s) = \frac{1}{T}\cdot\frac{1 - e^{-sT}}{s^2} \tag{39}$$

Therefore

$$V_b(s) = \frac{1}{TT_2}\cdot\frac{1 - e^{-sT}}{\left(s + \frac{1}{T_1}\right)\left(s + \frac{1}{T_2}\right)s} \tag{40}$$

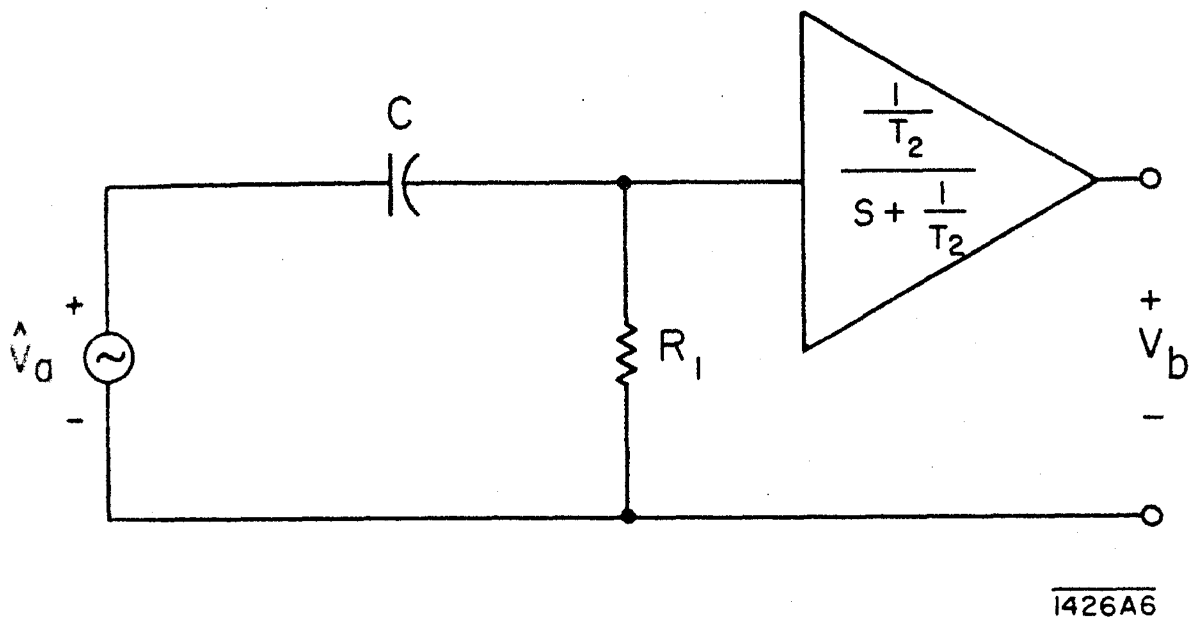

Fig. 6

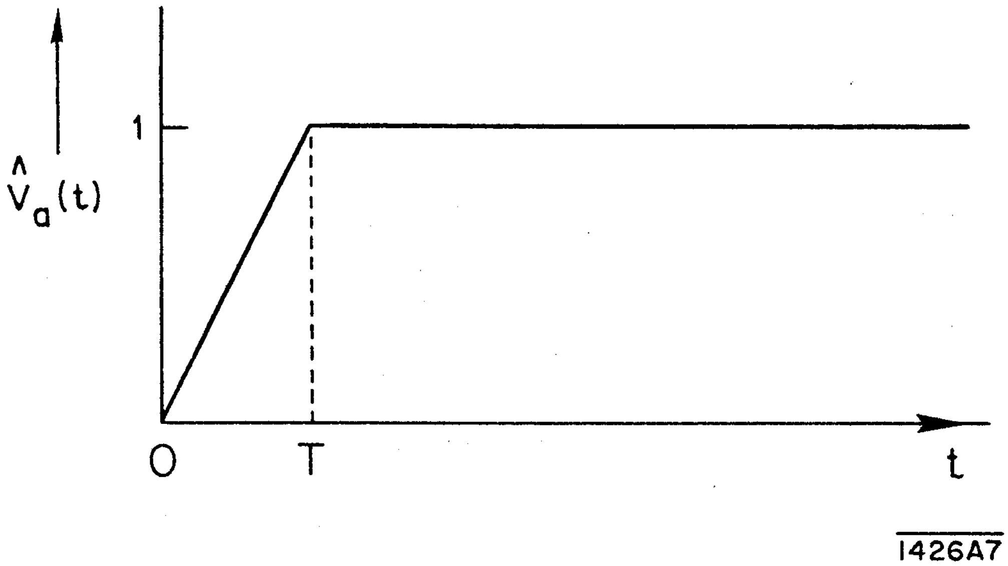

Fig. 7

For $0 \le t \le T$, we can write

$$V_b(s) = \frac{1}{TT_2} \cdot \frac{1}{s\left(s+\frac{1}{T_1}\right)\left(s+\frac{1}{T_2}\right)}$$

$$= \frac{1}{TT_2}\left\{\frac{T_1T_2}{s} + \frac{\frac{T_1^2T_2}{T_2-T_1}}{s+\frac{1}{T_1}} + \frac{\frac{T_1T_2^2}{T_1-T_2}}{s+\frac{1}{T_2}}\right\} \tag{41}$$

Hence,

$$v_b(t) = \frac{1}{TT_2}\left\{T_1T_2 + \frac{T_1^2T_2}{T_2-T_1}\, e^{-t/T_1} + \frac{T_1T_2^2}{T_1-T_2}\, e^{-t/T_2}\right\}$$

$$= \frac{T_1}{T} + \frac{T_1^2}{T(T_2-T_1)}\, e^{-t/T_1} + \frac{T_1T_2}{T(T_1-T_2)}\, e^{-t/T_2}$$

$$0 \le t \le T \tag{42}$$

For $T \le t < \infty$, we obtain

$$V_b(s) = \frac{1}{TT_2} \cdot \frac{1-e^{-sT}}{s\left(s+\frac{1}{T_1}\right)\left(s+\frac{1}{T_2}\right)}$$

$$= \frac{1}{TT_2}\left\{\frac{\frac{T_1^2T_2\left(1-e^{T/T_1}\right)}{T_2-T_1}}{s+\frac{1}{T_1}} + \frac{\frac{T_1T_2^2\left(1-e^{T/T_2}\right)}{T_1-T_2}}{s+\frac{1}{T_2}}\right\} \tag{43}$$

Hence

$$v_b(t) = \frac{T_1^2}{T(T_1 - T_2)} \left(e^{T/T_1} - 1\right) e^{-t/T_1}$$

$$- \frac{T_1 T_2}{T_1 - T_2} \left(e^{T/T_2} - 1\right) e^{-t/T_2}$$

$$T \leq t < \infty \qquad (44)$$

$v_b(t)$ has been tabulated as a function of time for various values of T_1 and T_2 on the IBM 360/91. The FORTRAN program listing is given in Appendix I. Figure 8 shows one plot of $v_b(t)$ for some selected values of T_1 and T_2. A more extensive tabulation will be found in Appendix II.

It should be noted that the shape of the output pulse shown in Fig. 8 is similar in form to that obtained experimentally using the multiwire chamber built by the Counting Electronics Group at SLAC. We observe from Fig. 8 that for a specified amplifier bandwidth $(1/T_2)$, the output pulse rises faster with a decrease in the input differentiating circuit time constant $T_1 = RC$. This is coupled with an increase in the maximum value of the output pulse and a corresponding increase in the pulse width. Increase in the pulse width implies that the resolving time of the counter is also increased. Alternately, we can conclude from this figure that for a given input circuit time constant T_1, increase in amplifier bandwidth results in a pulse with a faster rise time, higher amplitude and shorter pulse duration.

Our analysis so far assumed that the voltage $v_a(t)$ is always the same for each event, i.e., has the same rise time each time primary ionization takes place. Under this idealized situation, it is evident that it is best to have an amplifier with infinite bandwidth. However, as it will be pointed out later, in practice the rise time of $v_a(t)$ will vary to some extent from event to event. It would be thus profitable to examine the effect of a non-ideal amplifier (amplifier with finite bandwidth) along with the input differentiating circuit on input pulses of identical final heights but different rise times. For simplicity, consider only two types

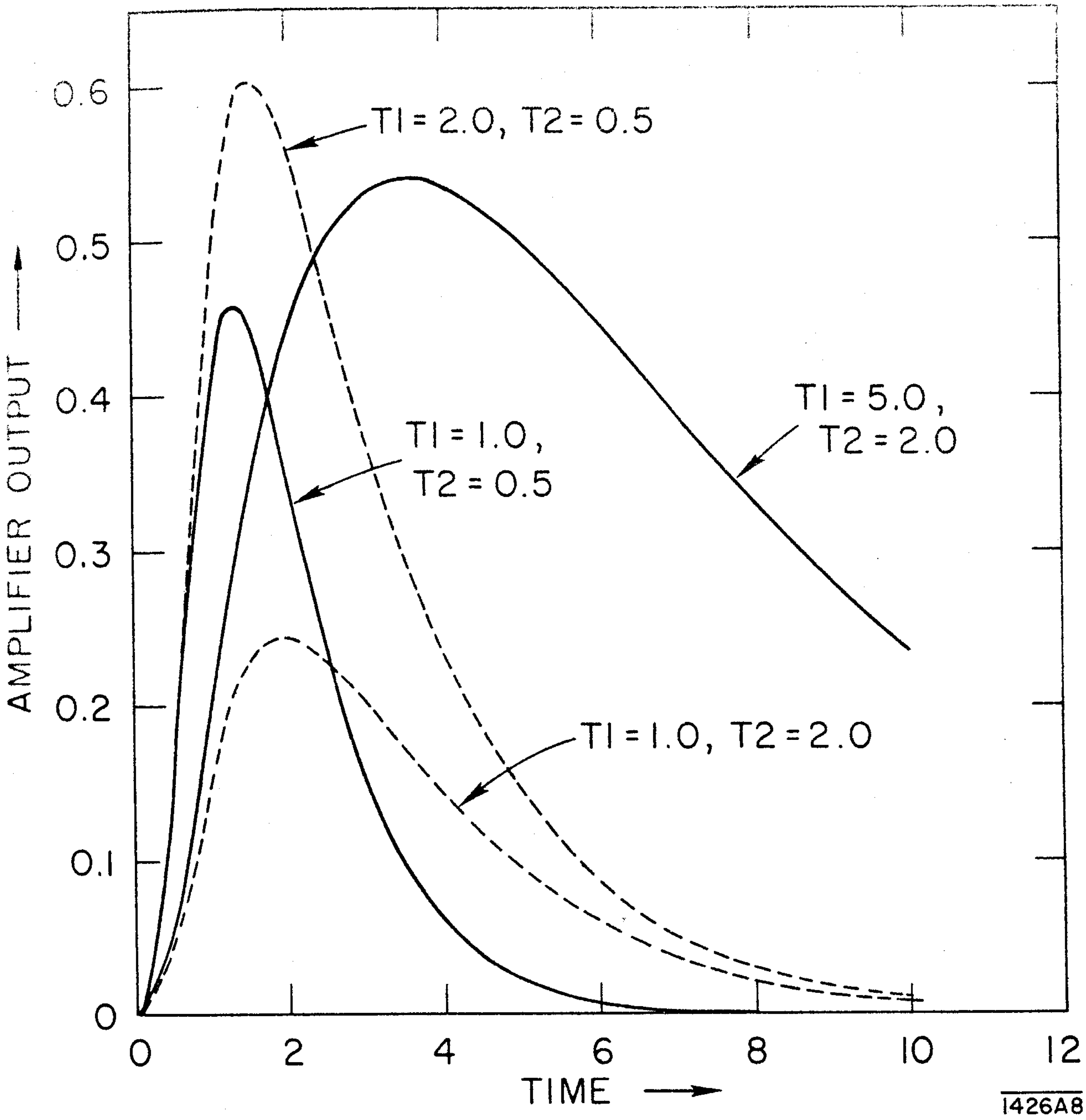
AMPLIFIER OUTPUT
0.6
0.5
0.4
0.3
0.2
0.1
0
T1 = 2.0, T2 = 0.5
T1 = 5.0, T2 = 2.0
T1 = 1.0, T2 = 0.5
T1 = 1.0, T2 = 2.0
0
2
4
6
8
10
12
TIME
1426A8

Fig. 8

of input pulses:

$$\hat{v}'_a(t) = u(t) \tag{45}$$

$$\hat{v}''_a(t) = \frac{1}{T}\left\{t\,u(t) - (t-T)\,u\,(t-T)\right\} \tag{46}$$

Assume first that the amplifier is an ideal amplifier, i.e., has an infinite bandwidth. In this case the amplifier output will be the same as that obtained at the input of the amplifier, i.e., the voltage $v_R(t)$ across the resistor R in Fig. 6. For $\hat{v}'_a(t)$ as the input pulse, the voltage $v'_R(t)$ across R is given as:

$$v'_R(t) = e^{-t/T_1} \tag{47}$$

Maximum value of $v'_R(t)$ is at t=0 and is equal to 1. In the second case, with $\hat{v}''_a(t)$ as the input pulse, the voltage $v''_R(t)$ across R is

$$v''_R(t) = \begin{cases} \frac{T_1}{T}\left(1 - e^{-t/T_1}\right) & 0 \le t \le T \quad (48) \\ \frac{T_1}{T}\left(e^{T/T_1} - 1\right) e^{-t/T_1} & T \le t < \infty \quad (49) \end{cases}$$

Maximum value of $v''_R(t)$ is at t=T and is given by $T_1/T\left[\left(1 - e^{-T/T_1}\right)\right]$ which is equal to $1 - e^{-1} = 0.63$ for $T = T_1$. Thus the output pulse height varies from 1 to 0.63 in the case of an ideal amplifier.

We now consider the effect of finite amplifier bandwidths and assume the amplifier to be described by a transfer function $1/T_2\left(s + (1/T_2)\right)$. The amplifier output $v'_b(t)$ for an input $\hat{v}'_a(t)$ is given by

$$v'_b(t) = \frac{t}{T_1}\,e^{-t/T_1} \tag{50}$$

if $T_1 = T_2$. $v'_b(t)$ has a maximum at $t = T_1$ and the maximum amplitude is 1/e. Whereas, for $v''_a(t)$ as input, the output $v''_b(t)$ of the amplifier is

$$v''_b(t) = \frac{1}{T}\left[(e-1)\,t - T\right]\,e^{-t/T} \qquad t \ge T \tag{51}$$

for $T_1 = T_2 = T$. Since for $t \leq T$, the output $v_R''(t)$ of the input differentiating circuit is given by Eq. (48). This voltage (which has a positive rate of change) being fed into the amplifier, the amplifier output can never exceed the input voltage when the latter is increasing. As a result, the rate of change of output voltage is also positive for $t \leq T$. Thus, it follows that the maximum value of the amplifier output $v_b''(t)$ is achieved for $t > T$. It can be shown from Eq. (51), the maximum value of $v_b''(t)$ occurs at $t = eT/(e-1)$ and is given by

$$e^{-1} (e-1) \cdot \exp\left[-\frac{1}{e-1}\right] = (0.962)\, e^{-1}$$

Consequently, there is very little spread in the height of the output pulses in the case of a non-ideal amplifier.

We can thus conclude that from the point of view of minimizing the spread of the heights of output pulses, it is preferable to use an amplifier with a finite bandwidth. The inverse bandwidth T_2 of the amplifier should be made equal to the time constant T_1 of the input differentiating circuit which in turn should be equal to the average rise time of the input pulse. Another advantage of reducing the amplifier bandwidth is the associated reduction in amplifier noise.

D. Discussion

An analytical expression for the input pulse generated at the anode has been derived along with an approximate expression for the amplifier output pulse [Eqs. (21), (42) and (44)] . The derivation was based on the assumption that all the primary electrons are collected instantaneously by the anode and the secondary ionization takes place in the immediate neighborhood of the wire. The output pulse is thus assumed to be determined exclusively by the motion of the positive ions and each pulse will have the same shape regardless of the location of the primary ionization. However, if electronegative impurities like oxygen are present inside the chamber, electrons would be rapidly captured to form heavy negative ions having the same mobility as the positive ions. The drift velocities of these heavy negative ions differ by a factor of 1000 from that of the free electrons. Consequently rise time of the output pulse will be almost 1000 times longer than that would be obtained in the idealized case. Thus short clipping time T_1 cannot be used with the result that the resolving time of the chamber will be significantly increased. It should be noted that oxygen is likely contaminant in any chamber because of leaks, air absorption in the chamber walls and insufficient evacuation. If pure argon is used as the chamber gas than it is preferable to keep the voltage across the electrodes as low as possible to facilitate better electron collection by the wires. On the other hand, lower collective voltage results in a lower gas multiplication factor M reducing the height of the output pulse. A better way to improve electron collection and also increase M, is to mix a small percentage of some polyatomic gases like CO_2 to the chamber gas. For example addition of 5 - 10% of CO_2 would increase the electron drift velocity almost ten times for a fixed collecting voltage and a fixed gas pressure. There are several other associated advantages when gas mixtures are used instead of pure gases. These polyatomic gases act as a self-quencher in the case of a spark breakdown. In a pure noble gas, the electrons may diffuse to the side of the chamber due to high electron energy and thus not follow the field lines. Addition of CO_2 greatly reduces the diffusion effects by lowering the electron energy and increasing the drift velocities. Minimization of diffusion effects enhances pulse profile studies. Often the electron collection may be enhanced by purposely stimulating a spark by increasing the collecting voltage for example. The spark will stop as soon as all of the electrons have been collected. Faster electron collection also minimizes the possibility of recombination with the slower moving positive ions.

Determination of positive ion mobility in gas mixtures is fairly complicated. For initial estimates of pulse sizes and rise times, it is usually sufficient to use the ion mobility for the predominant gas as that of the gas mixture.[11]

We mentioned earlier the advantages of adding a polyatomic gas to a noble gas and use the gas mixture as the chamber gas. CO_2 is a commonly used stabilizing gas. Other gases in this class are N_2, methane and carbon tetrachloride. In some respect $Ar-CO_2$ mixture is not preferable. Pure argon is attractive as a chamber gas. This is because, in pure argon, the amount of energy (W) which a particle loses on the average to form one ion pair stays fairly constant. However, in an $Ar-CO_2$ mixture W value is not constant and thus may lead to output pulses of varying heights (N_p will not be constant). For similar reasons methane is not preferable. On the other hand, both Ar and N_2 have constant W values and their mixture may be expected to have a constant W value. Hence $Ar-N_2$ mixture may be a more appropriate chamber gas. Suitable proportions would be 90% argon and 10% nitrogen.[11] Another recommended gas mixture is 96% helium and 4% isobutane.[5] It can be pointed out here that satisfactory results have also been obtained using 80% argon and 20% isobutane gas mixture.[12] Note that helium has a positive ionic mobility which is five times greater than that of argon and nitrogen. Equation (21) indicates that a higher mobility would result in output pulses having a faster rise time which would be preferable if shorter resolving time is desired.

Effect of straggling on the pulse shape was neglected by assuming that all electrons are being formed under identical electrical conditions. However, the field near the wire does change very rapidly. Thus strictly speaking, some amount of straggling will be introduced because the electrons cannot remain in equilibrium with the field. Effect of straggling is to vary the rise times of the pulses.

We have also neglected the capacitive coupling between wires. It appears that the pulse induced by positive ion movement near one wire would result in pulses of the same polarity on adjacent wires. Fortunately, as Charpak[12] has pointed out, charge induced on one wire by the positive ion movement is equal and opposite to the charge induced on all other conductors including the cathode. This opposed coupling would create pulses of opposite signs in adjacent wires and in effect would cancel the pulses created by capacitive coupling.

Several other comments are here in order. Excited ions or molecules or atoms would often create photons, which in turn may cause liberation of photoelectrons from the gas and the cathode. These secondary avalanches are hard to distinguish from the primary avalanches as they follow closely each other, and in effect increase the gas multiplication significantly, often leading to instability. Photoelectrons are also liberated by the positive ions as they hit the outer electrodes. These discharges trail the primary discharge by t_+, the collection time of the positive ions. Effect of this second type of discharge is again to increase the gas multiplication factor and may give double or multiple pulses if the time constants in the amplifier are not quite long. These secondary effects can be significantly reduced by additional small amounts of any molecular gas like CO_2, N_2, etc.

REFERENCES

1. G. Charpak et al., Nucl. Instr. and Methods 62, 262 (1968).
2. G. Amato and G. Petrucci, "A beam profile analyzer using proportional multiwire chamber," Report No. CERN 68-33 (August 1968).
3. R. S. Larsen, "Proportional wire chamber profile monitor," SLAC memorandum, Stanford Linear Accelerator Center, Stanford University, Stanford, California (March 10, 1969).
4. D. H. Wilkinson, Ionization Chambers and Counters, (Cambridge University Press, London, 1950); Ch. 4.
5. W. J. Price, Nuclear Radiation Detection, (McGraw-Hill Co., Inc., New York, 1958); Chs. 4, 5, and 6.
6. W. R. Smythe, Static and Dynamic Electricity, 2nd Edition (McGraw-Hill Co., Inc., New York, 1950); p. 34.
7. S. Ramo and J. R. Whinnery, Fields and Waves in Modern Radio, 2nd Edition (John Wiley and Sons, New York, 1962); p. 75.
8. National Research Counsel, International Critical Tables of Numerical Data, Physics, Chemistry and Technology (McGraw-Hill Co., Inc., New York, 1929); Vol. VI.
9. Emde Jahnke and Friedrich Losch, Tables of Higher Functions, 6th Edition (McGraw-Hill Co., Inc., New York, 1960); p. 23.
10. A. B. Gillespie, Signal, Noise and Resolution in Nuclear Counter Amplifiers, (Pergamon Press, New York, 1953).
11. R. Wilson, "Ionization counters," in Techniques of High Energy Physics, D. M. Ritson, Editor, (Interscience Publishers, New York, 1961); pp. 271-299.
12. G. Charpak, "Development of multiwire proportional chambers," CERN Courier, Vol. 9, No. 6 (June 1969); pp. 174-176.

```
LEVEL 16 ( 1 JULY 68)                              OS/360  FORTRAN H

        COMPILER OPTIONS - NAME=  MAIN,OPT=00,LINECNT=58,SOURCE,EBCDIC,LIST,NODE
                C
                C   EVALUATION OF AMPLIFIER OUTPUT VOLTAGE FOR
                C   VARIOUS VALUES OF INPUT CIRCUIT TIME CONSTANT
                C   ( T1  ) AND AMPLIFIER BANDWIDTH  ( 1/T2)
                C
  ISN 0002              DIMENSION VBC(100), YT(100)
  ISN 0003            3  READ (5,5,END=150) T1, T2
  ISN 0004             5 FORMAT (8F10.0)
                C
                C   CALCULATION FOR TIME YT  LESS THAN OR EQUAL TO  1
                C
  ISN 0005              Y = 0.0
  ISN 0006              DO 10 I = 1,6
  ISN 0007              A = T1*T1*EXP(- Y/T1)/(T1 - T2)
  ISN 0008              B = T1*T2*EXP(-Y/T2)/(T1 - T2)
  ISN 0009              VBC(I) = T1 - A + B
  ISN 0010              YT(I) = Y
  ISN 0011           10 Y = Y +0.2
                C
                C   CALCULATION FOR TIME  YT  GREATER THAN  1
                C
  ISN 0012              Z = 1.2
  ISN 0013              DO 20  I = 1,46
  ISN 0014              A = T1*T1*(EXP(1.0/T1) - 1.0)
  ISN 0015              A = A*EXP(-Z/T1)/(T1 - T2)
  ISN 0016              B = T1*T2*(EXP(1.0/T2) - 1.0)
  ISN 0017              B = B*EXP(- Z/T2)/(T1 - T2)
  ISN 0018              K = I + 6
  ISN 0019              VBC(K) = A - B
  ISN 0020              YT(K) = Z
  ISN 0021           20 Z = Z + 0.2
  ISN 0022              PRINT 30, T1, T2
  ISN 0023           30 FORMAT (14H1 T1  T2  ARE , 2E14.3)
  ISN 0024              PRINT 31
  ISN 0025           31 FORMAT (40H0              TIME                 OUTPUT       )
  ISN 0026              PRINT 33
  ISN 0027           33 FORMAT (1H0)
  ISN 0028              DO 40  I = 1, 51
  ISN 0029           40 PRINT 32, YT(I), VBC(I)
  ISN 0030           32 FORMAT (E20.2, E20.4) .
  ISN 0031              GO TO 3
  ISN 0032          150  RETURN
  ISN 0033              END
```

T1 T2 ARE 0.100E 00 0.500E 00

TIME	OUTPUT
0.0	-0.5960E-07
0.20E 00	0.1959E-01
0.40E 00	0.4429E-01
0.60E 00	0.6241E-01
0.80E 00	0.7477E-01
0.10E 01	0.8308E-01
0.12E 01	0.6907E-01
0.14E 01	0.4811E-01
0.16E 01	0.3249E-01
0.18E 01	0.2181E-01
0.20E 01	0.1463E-01
0.22E 01	0.9805E-02
0.24E 01	0.6573E-02
0.26E 01	0.4406E-02
0.28E 01	0.2953E-02
0.30E 01	0.1980E-02
0.32E 01	0.1327E-02
0.34E 01	0.8895E-03
0.36E 01	0.5962E-03
0.38E 01	0.3997E-03
0.40E 01	0.2679E-03
0.42E 01	0.1796E-03
0.44E 01	0.1204E-03
0.46E 01	0.8069E-04
0.48E 01	0.5409E-04
0.50E 01	0.3626E-04
0.52E 01	0.2430E-04
0.54E 01	0.1629E-04
0.56E 01	0.1092E-04
0.58E 01	0.7320E-05
0.60E 01	0.4907E-05
0.62E 01	0.3289E-05
0.64E 01	0.2205E-05
0.66E 01	0.1478E-05
0.68E 01	0.9907E-06
0.70E 01	0.6641E-06
0.72E 01	0.4452E-06
0.74E 01	0.2984E-06
0.76E 01	0.2000E-06
0.78E 01	0.1341E-06
0.80E 01	0.8988E-07
0.82E 01	0.6025E-07
0.84E 01	0.4038E-07
0.86E 01	0.2707E-07
0.88E 01	0.1815E-07
0.90E 01	0.1216E-07
0.92E 01	0.8153E-08
0.94E 01	0.5465E-08
0.96E 01	0.3664E-08
0.98E 01	0.2456E-08
0.10E 02	0.1646E-08

T1 T2 ARE 0.100E 00 0.100E 01

TIME	OUTPUT
0.0	0.0
0.20E 00	0.1053E-01
0.40E 00	0.2572E-01
0.60E 00	0.3905E-01
0.80E 00	0.5008E-01
0.10E 01	0.5912E-01
0.12E 01	0.5600E-01
0.14E 01	0.4688E-01
0.16E 01	0.3852E-01
0.18E 01	0.3156E-01
0.20E 01	0.2584E-01
0.22E 01	0.2115E-01
0.24E 01	0.1732E-01
0.26E 01	0.1418E-01
0.28E 01	0.1161E-01
0.30E 01	0.9505E-02
0.32E 01	0.7782E-02
0.34E 01	0.6372E-02
0.36E 01	0.5217E-02
0.38E 01	0.4271E-02
0.40E 01	0.3497E-02
0.42E 01	0.2863E-02
0.44E 01	0.2344E-02
0.46E 01	0.1919E-02
0.48E 01	0.1571E-02
0.50E 01	0.1286E-02
0.52E 01	0.1053E-02
0.54E 01	0.8623E-03
0.56E 01	0.7060E-03
0.58E 01	0.5780E-03
0.60E 01	0.4732E-03
0.62E 01	0.3875E-03
0.64E 01	0.3172E-03
0.66E 01	0.2597E-03
0.68E 01	0.2126E-03
0.70E 01	0.1741E-03
0.72E 01	0.1425E-03
0.74E 01	0.1167E-03
0.76E 01	0.9555E-04
0.78E 01	0.7823E-04
0.80E 01	0.6405E-04
0.82E 01	0.5244E-04
0.84E 01	0.4293E-04
0.86E 01	0.3515E-04
0.88E 01	0.2878E-04
0.90E 01	0.2356E-04
0.92E 01	0.1929E-04
0.94E 01	0.1579E-04
0.96E 01	0.1293E-04
0.98E 01	0.1059E-04
0.10E 02	0.8668E-05

T1 T2 ARE 0.100E 00 0.100E 02

TIME	OUTPUT
0.0	0.0
0.20E 00	0.1127E-02
0.40E 00	0.2969E-02
0.60E 00	0.4875E-02
0.80E 00	0.6756E-02
0.10E 01	0.8602E-02
0.12E 01	0.9285E-02
0.14E 01	0.9217E-02
0.16E 01	0.9050E-02
0.18E 01	0.8873E-02
0.20E 01	0.8698E-02
0.22E 01	0.8525E-02
0.24E 01	0.8357E-02
0.26E 01	0.8191E-02
0.28E 01	0.8029E-02
0.30E 01	0.7870E-02
0.32E 01	0.7714E-02
0.34E 01	0.7561E-02
0.36E 01	0.7412E-02
0.38E 01	0.7265E-02
0.40E 01	0.7121E-02
0.42E 01	0.6980E-02
0.44E 01	0.6842E-02
0.46E 01	0.6706E-02
0.48E 01	0.6574E-02
0.50E 01	0.6443E-02
0.52E 01	0.6316E-02
0.54E 01	0.6191E-02
0.56E 01	0.6068E-02
0.58E 01	0.5948E-02
0.60E 01	0.5830E-02
0.62E 01	0.5715E-02
0.64E 01	0.5602E-02
0.66E 01	0.5491E-02
0.68E 01	0.5382E-02
0.70E 01	0.5275E-02
0.72E 01	0.5171E-02
0.74E 01	0.5069E-02
0.76E 01	0.4968E-02
0.78E 01	0.4870E-02
0.80E 01	0.4773E-02
0.82E 01	0.4679E-02
0.84E 01	0.4586E-02
0.86E 01	0.4495E-02
0.88E 01	0.4406E-02
0.90E 01	0.4319E-02
0.92E 01	0.4234E-02
0.94E 01	0.4150E-02
0.96E 01	0.4068E-02
0.98E 01	0.3987E-02
0.10E 02	0.3908E-02

T1 T2 ARE 0.500E 00 0.100E 00

TIME	OUTPUT
0.0	0.0
0.20E 00	0.9797E-01
0.40E 00	0.2215E 00
0.60E 00	0.3121E 00
0.80E 00	0.3739E 00
0.10E 01	0.4154E 00
0.12E 01	0.3453E 00
0.14E 01	0.2405E 00
0.16E 01	0.1625E 00
0.18E 01	0.1091E 00
0.20E 01	0.7313E-01
0.22E 01	0.4902E-01
0.24E 01	0.3286E-01
0.26E 01	0.2203E-01
0.28E 01	0.1477E-01
0.30E 01	0.9898E-02
0.32E 01	0.6635E-02
0.34E 01	0.4447E-02
0.36E 01	0.2981E-02
0.38E 01	0.1998E-02
0.40E 01	0.1340E-02
0.42E 01	0.8979E-03
0.44E 01	0.6019E-03
0.46E 01	0.4035E-03
0.48E 01	0.2705E-03
0.50E 01	0.1813E-03
0.52E 01	0.1215E-03
0.54E 01	0.8146E-04
0.56E 01	0.5460E-04
0.58E 01	0.3660E-04
0.60E 01	0.2454E-04
0.62E 01	0.1645E-04
0.64E 01	0.1102E-04
0.66E 01	0.7390E-05
0.68E 01	0.4954E-05
0.70E 01	0.3320E-05
0.72E 01	0.2226E-05
0.74E 01	0.1492E-05
0.76E 01	0.1000E-05
0.78E 01	0.6704E-06
0.80E 01	0.4494E-06
0.82E 01	0.3012E-06
0.84E 01	0.2019E-06
0.86E 01	0.1354E-06
0.88E 01	0.9073E-07
0.90E 01	0.6082E-07
0.92E 01	0.4077E-07
0.94E 01	0.2733E-07
0.96E 01	0.1832E-07
0.98E 01	0.1228E-07
0.10E 02	0.8231E-08

T1 T2 ARE 0.500E 00 0.200E 01

TIME	OUTPUT
0.0	0.0
0.20E 00	0.8495E-02
0.40E 00	0.2907E-01
0.60E 00	0.5632E-01
0.80E 00	0.8677E-01
0.10E 01	0.1182E 00
0.12E 01	0.1408E 00
0.14E 01	0.1500E 00
0.16E 01	0.1509E 00
0.18E 01	0.1467E 00
0.20E 01	0.1396E 00
0.22E 01	0.1309E 00
0.24E 01	0.1215E 00
0.26E 01	0.1120E 00
0.28E 01	0.1027E 00
0.30E 01	0.9386E-01
0.32E 01	0.8555E-01
0.34E 01	0.7782E-01
0.36E 01	0.7069E-01
0.38E 01	0.6415E-01
0.40E 01	0.5817E-01
0.42E 01	0.5272E-01
0.44E 01	0.4776E-01
0.46E 01	0.4325E-01
0.48E 01	0.3916E-01
0.50E 01	0.3545E-01
0.52E 01	0.3209E-01
0.54E 01	0.2904E-01
0.56E 01	0.2628E-01
0.58E 01	0.2379E-01
0.60E 01	0.2153E-01
0.62E 01	0.1948E-01
0.64E 01	0.1763E-01
0.66E 01	0.1595E-01
0.68E 01	0.1443E-01
0.70E 01	0.1306E-01
0.72E 01	0.1182E-01
0.74E 01	0.1069E-01
0.76E 01	0.9675E-02
0.78E 01	0.8754E-02
0.80E 01	0.7921E-02
0.82E 01	0.7167E-02
0.84E 01	0.6485E-02
0.86E 01	0.5868E-02
0.88E 01	0.5310E-02
0.90E 01	0.4804E-02
0.92E 01	0.4347E-02
0.94E 01	0.3934E-02
0.96E 01	0.3559E-02
0.98E 01	0.3221E-02
0.10E 02	0.2914E-02

T1 T2 ARE 0.500E 00 0.100E 02

I

TIME	OUTPUT
0.0	0.0
0.20E 00	0.1746E-02
0.40E 00	0.6146E-02
0.60E 00	0.1226E-01
0.80E 00	0.1946E-01
0.10E 01	0.2733E-01
0.12E 01	0.3384E-01
0.14E 01	0.3790E-01
0.16E 01	0.4032E-01
0.18E 01	0.4164E-01
0.20E 01	0.4224E-01
0.22E 01	0.4236E-01
0.24E 01	0.4216E-01
0.26E 01	0.4175E-01
0.28E 01	0.4121E-01
0.30E 01	0.4059E-01
0.32E 01	0.3992E-01
0.34E 01	0.3921E-01
0.36E 01	0.3849E-01
0.38E 01	0.3777E-01
0.40E 01	0.3705E-01
0.42E 01	0.3633E-01
0.44E 01	0.3562E-01
0.46E 01	0.3493E-01
0.48E 01	0.3424E-01
0.50E 01	0.3357E-01
0.52E 01	0.3290E-01
0.54E 01	0.3225E-01
0.56E 01	0.3162E-01
0.58E 01	0.3099E-01
0.60E 01	0.3038E-01
0.62E 01	0.2978E-01
0.64E 01	0.2919E-01
0.66E 01	0.2861E-01
0.68E 01	0.2804E-01
0.70E 01	0.2749E-01
0.72E 01	0.2694E-01
0.74E 01	0.2641E-01
0.76E 01	0.2589E-01
0.78E 01	0.2537E-01
0.80E 01	0.2487E-01
0.82E 01	0.2438E-01
0.84E 01	0.2390E-01
0.86E 01	0.2342E-01
0.88E 01	0.2296E-01
0.90E 01	0.2250E-01
0.92E 01	0.2206E-01
0.94E 01	0.2162E-01
0.96E 01	0.2119E-01
0.98E 01	0.2077E-01
0.10E 02	0.2036E-01

T1 T2 ARE 0.10CE C1 C.1CCE CC

TIME	CUTPUT
C.C	C.3576E-C6
C.20E C0	C.1C53E CC
C.40E C0	C.2572E CC
C.6CE CC	0.39C5E 0C
C.8CE CC	C.5C08E CC
C.10E 01	C.5913E C0
C.12E C1	C.56C0E C0
C.14E C1	C.4688E CC
C.16E 01	C.3852E C0
C.18E 01	0.3155E CC
C.20E C1	0.2584E C0
C.22E C1	C.2115E CC
C.24E C1	0.1732E 0C
C.26E C1	0.1418E CC
C.28E C1	C.1161E CC
0.30E 01	C.9505E-C1
C.32E C1	C.7782E-C1
C.34E C1	0.6372E-C1
C.36E C1	C.5217E-01
C.38E C1	0.4271E-C1
C.40E C1	C.3497E-C1
C.42E 01	C.2863E-C1
C.44E C1	0.2344E-C1
C.46E C1	0.1919E-C1
C.48E 01	C.1571E-C1
C.5CE C1	C.1286E-C1
C.52E C1	0.1C53E-C1
C.54E C1	C.8623E-C2
C.56E C1	C.7C6CE-C2
C.58E C1	C.578CE-C2
C.60E C1	C.4732E-C2
C.62E C1	C.3875E-C2
C.64E C1	C.3172E-C2
C.66E 01	C.2597E-C2
C.68E C1	C.2126E-02
C.70E C1	C.1741E-02
C.72E 01	0.1425E-C2
C.74E C1	C.1167E-C2
C.76E C1	C.9555E-03
C.78E C1	C.7823E-03
C.80E C1	C.6405E-C3
C.82E 01	C.5244E-03
C.84E C1	C.4293E-03
C.86E C1	0.3515E-C3
C.88E 01	C.2878E-C3
C.9CE C1	C.2356E-C3
C.92E C1	C.1929E-03
C.94E C1	C.1579E-03
C.96E C1	C.1293E-03
C.98E C1	C.1C59E-C3
C.10E C2	C.8668E-C4

T1 T2 ARE 0.100E 01 0.500E 00

TIME	OUTPUT
0.0	0.0
0.20E 00	0.3286E-01
0.40E 00	0.1087E 00
0.60E 00	0.2036E 00
0.80E 00	0.3032E 00
0.10E 01	0.3996E 00
0.12E 01	0.4555E 00
0.14E 01	0.4589E 00
0.16E 01	0.4334E 00
0.18E 01	0.3935E 00
0.20E 01	0.3481E 00
0.22E 01	0.3023E 00
0.24E 01	0.2592E 00
0.26E 01	0.2200E 00
0.28E 01	0.1854E 00
0.30E 01	0.1553E 00
0.32E 01	0.1295E 00
0.34E 01	0.1076E 00
0.36E 01	0.8913E-01
0.38E 01	0.7368E-01
0.40E 01	0.6050E-01
0.42E 01	0.5010E-01
0.44E 01	0.4123E-01
0.46E 01	0.3390E-01
0.48E 01	0.2785E-01
0.50E 01	0.2287E-01
0.52E 01	0.1876E-01
0.54E 01	0.1539E-01
0.56E 01	0.1262E-01
0.58E 01	0.1035E-01
0.60E 01	0.8479E-02
0.62E 01	0.6948E-02
0.64E 01	0.5692E-02
0.66E 01	0.4663E-02
0.68E 01	0.3820E-02
0.70E 01	0.3128E-02
0.72E 01	0.2562E-02
0.74E 01	0.2098E-02
0.76E 01	0.1718E-02
0.78E 01	0.1407E-02
0.80E 01	0.1152E-02
0.82E 01	0.9434E-03
0.84E 01	0.7725E-03
0.86E 01	0.6325E-03
0.88E 01	0.5179E-03
0.90E 01	0.4240E-03
0.92E 01	0.3472E-03
0.94E 01	0.2842E-03
0.96E 01	0.2327E-03
0.98E 01	0.1905E-03
0.10E 02	0.1560E-03

T1 T2 ARE 0.100E 01 0.200E 01

TIME	OUTPUT
0.0	0.0
0.20E 00	0.9056E-02
0.40E 00	0.3286E-01
0.60E 00	0.6717E-01
0.80E 00	0.1087E 00
0.10E 01	0.1548E 00
0.12E 01	0.1945E 00
0.14E 01	0.2206E 00
0.16E 01	0.2361E 00
0.18E 01	0.2435E 00
0.20E 01	0.2448E 00
0.22E 01	0.2415E 00
0.24E 01	0.2349E 00
0.26E 01	0.2260E 00
0.28E 01	0.2155E 00
0.30E 01	0.2040E 00
0.32E 01	0.1919E 00
0.34E 01	0.1797E 00
0.36E 01	0.1675E 00
0.38E 01	0.1556E 00
0.40E 01	0.1441E 00
0.42E 01	0.1331E 00
0.44E 01	0.1227E 00
0.46E 01	0.1128E 00
0.48E 01	0.1036E 00
0.50E 01	0.9492E-01
0.52E 01	0.8689E-01
0.54E 01	0.7943E-01
0.56E 01	0.7254E-01
0.58E 01	0.6619E-01
0.60E 01	0.6034E-01
0.62E 01	0.5496E-01
0.64E 01	0.5003E-01
0.66E 01	0.4552E-01
0.68E 01	0.4139E-01
0.70E 01	0.3761E-01
0.72E 01	0.3417E-01
0.74E 01	0.3103E-01
0.76E 01	0.2816E-01
0.78E 01	0.2556E-01
0.80E 01	0.2319E-01
0.82E 01	0.2103E-01
0.84E 01	0.1907E-01
0.86E 01	0.1729E-01
0.88E 01	0.1567E-01
0.90E 01	0.1420E-01
0.92E 01	0.1287E-01
0.94E 01	0.1166E-01
0.96E 01	0.1056E-01
0.98E 01	0.9566E-02
0.10E 02	0.8664E-02

T1 T2 ARE 0.100E 01 0.100E 02

TIME	OUTPUT
0.0	0.0
0.20E 00	0.1861E-02
0.40E 00	0.6936E-02
0.60E 00	0.1457E-01
0.80E 00	0.2424E-01
0.10E 01	0.3550E-01
0.12E 01	0.4614E-01
0.14E 01	0.5451E-01
0.16E 01	0.6103E-01
0.18E 01	0.6605E-01
0.20E 01	0.6984E-01
0.22E 01	0.7263E-01
0.24E 01	0.7460E-01
0.26E 01	0.7592E-01
0.28E 01	0.7671E-01
0.30E 01	0.7706E-01
0.32E 01	0.7707E-01
0.34E 01	0.7680E-01
0.36E 01	0.7631E-01
0.38E 01	0.7564E-01
0.40E 01	0.7483E-01
0.42E 01	0.7392E-01
0.44E 01	0.7292E-01
0.46E 01	0.7185E-01
0.48E 01	0.7074E-01
0.50E 01	0.6959E-01
0.52E 01	0.6842E-01
0.54E 01	0.6724E-01
0.56E 01	0.6604E-01
0.58E 01	0.6485E-01
0.60E 01	0.6366E-01
0.62E 01	0.6248E-01
0.64E 01	0.6130E-01
0.66E 01	0.6014E-01
0.68E 01	0.5899E-01
0.70E 01	0.5786E-01
0.72E 01	0.5674E-01
0.74E 01	0.5564E-01
0.76E 01	0.5455E-01
0.78E 01	0.5349E-01
0.80E 01	0.5244E-01
0.82E 01	0.5142E-01
0.84E 01	0.5041E-01
0.86E 01	0.4941E-01
0.88E 01	0.4844E-01
0.90E 01	0.4749E-01
0.92E 01	0.4655E-01
0.94E 01	0.4563E-01
0.96E 01	0.4473E-01
0.98E 01	0.4385E-01
0.10E 02	0.4298E-01

T1 T2 ARE C.2CCE C1 C.1CCE CC

TIME	CUTPUT
C.C	0.3576E-C6
C.2CE CO	0.1C93F CO
C.4CE 00	C.2783E CO
C.60E CO	C.44C6E 00
C.80E CO	0.5888F CC
C.10E 01	C.7231E CC
C.12E 01	C.7353E CC
C.14E 01	C.6763E CC
C.16E C1	C.6134E CO
C.18E 01	C.5552E CO
C.20E C1	C.5C24E CC
C.22E C1	C.4546E CC
C.24E C1	C.4114E 00
C.26E 01	C.3722E CO
C.28E C1	0.3368E CC
C.30E C1	C.3C47E 00
C.32E C1	C.2757E CO
C.34E C1	C.2495E CC
C.36E C1	C.2258E CC
C.38E C1	0.2C43E CC
C.40E C1	C.1848E CC
C.42E C1	0.1672E CO
C.44E C1	C.1513E CO
C.46E C1	C.1369E CO
C.48E C1	C.1239E CC
C.50E C1	C.1121E CC
C.52E C1	0.1014E CC
C.54E C1	C.9178E-C1
C.56E C1	C.8305E-C1
C.58E C1	C.7515E-01
C.60E 01	C.68C0E-01
0.62E C1	C.6153E-C1
C.64E C1	C.5567E-01
C.66E C1	C.5037E-01
C.68E C1	0.4558E-C1
C.70E C1	0.4124E-01
C.72E C1	C.3732E-C1
C.74E C1	C.3377E-01
C.76E C1	0.3055E-C1
C.78E 01	0.2765E-C1
0.80E C1	0.25C1E-01
C.82E C1	C.2263E-C1
C.84E C1	C.2C48E-C1
C.86E C1	C.1853E-C1
C.88E C1	C.1677E-C1
C.9CE 01	0.1517E-01
C.92E C1	0.1373E-C1
C.94E 01	0.1242E-C1
C.96E C1	C.1124E-01
C.98E C1	C.1C17E-C1
C.10E C2	C.9202E-C2

T1 T2 ARE C.2CCE C1 C.5CCE CC

TIME	CUTPUT
C.C	0.5960E-C6
C.20E 0C	0.3398E-01
C.4CE C0	C.1163E 00
C.6CE C0	C.2253E 0C
C.80E 00	0.3471E CC
C.10E 01	0.4728E CC
C.12E C1	C.5630E C0
C.14E C1	C.6CCCE C0
C.16E C1	C.6C37E CC
C.18E C1	C.5870E C0
C.20E C1	0.5584E C0
C.22E 01	0.5235E C0
C.24E C1	C.4860E 00
C.26E C1	0.4480E 00
C.28E C1	C.41C8E 0C
C.30E 01	C.3754E 0C
C.32E C1	0.3422E CC
C.34E C1	C.3113E CC
C.36E 01	C.2828E 0C
C.38E C1	0.2566E C0
C.4CE C1	C.2327E 00
C.42E C1	C.21C9E CC
C.44E 01	C.191CE CC
C.46E C1	C.1730E 00
C.48E C1	0.1566E C0
C.50E C1	C.1418E 00
C.52E C1	0.1284E CC
C.54E C1	C.1162E 0C
C.56E C1	C.1051E C0
0.58E C1	C.9515E-01
C.60E C1	C.861CE-01
C.62E C1	0.7791E-01
C.64E C1	C.7050E-01
C.66E C1	C.638CE-C1
C.68E C1	C.5773E-C1
C.70E C1	C.5224E-C1
C.72E 01	C.4727E-01
C.74E C1	C.4277E-C1
C.76E C1	C.3870E-C1
C.78E C1	C.35C2E-01
C.80E C1	C.3168E-01
C.82E C1	C.2867E-01
C.84E C1	C.2594E-C1
C.86E C1	0.2347E-C1
C.88E C1	0.2124E-01
C.9CE C1	C.1922E-01
C.92E C1	C.1739E-C1
C.94E C1	C.1573E-C1
C.96E 01	C.1424E-01
C.98E C1	C.1288E-C1
C.10E 02	C.1166E-01

T1 T2 ARE 0.200E 01 0.100E 01

TIME	OUTPUT
0.0	0.0
0.20E 00	0.1811E-01
0.40E 00	0.6572E-01
0.60E 00	0.1343E 00
0.80E 00	0.2174E 00
0.10E 01	0.3096E 00
0.12E 01	0.3890E 00
0.14E 01	0.4411E 00
0.16E 01	0.4721E 00
0.18E 01	0.4869E 00
0.20E 01	0.4895E 00
0.22E 01	0.4830E 00
0.24E 01	0.4698E 00
0.26E 01	0.4519E 00
0.28E 01	0.4309E 00
0.30E 01	0.4079E 00
0.32E 01	0.3838E 00
0.34E 01	0.3594E 00
0.36E 01	0.3350E 00
0.38E 01	0.3112E 00
0.40E 01	0.2883E 00
0.42E 01	0.2662E 00
0.44E 01	0.2453E 00
0.46E 01	0.2256E 00
0.48E 01	0.2071E 00
0.50E 01	0.1898E 00
0.52E 01	0.1738E 00
0.54E 01	0.1589E 00
0.56E 01	0.1451E 00
0.58E 01	0.1324E 00
0.60E 01	0.1207E 00
0.62E 01	0.1099E 00
0.64E 01	0.1001E 00
0.66E 01	0.9103E-01
0.68E 01	0.8277E-01
0.70E 01	0.7523E-01
0.72E 01	0.6834E-01
0.74E 01	0.6205E-01
0.76E 01	0.5633E-01
0.78E 01	0.5112E-01
0.80E 01	0.4637E-01
0.82E 01	0.4206E-01
0.84E 01	0.3814E-01
0.86E 01	0.3458E-01
0.88E 01	0.3134E-01
0.90E 01	0.2840E-01
0.92E 01	0.2574E-01
0.94E 01	0.2332E-01
0.96E 01	0.2112E-01
0.98E 01	0.1913E-01
0.10E 02	0.1733E-01

T1 T2 ARE 0.200E 01 0.100E 02

TIME	OUTPUT
0.0	0.0
0.20E 00	0.1922E-02
0.40E 00	0.7393E-02
0.60E 00	0.1600E-01
0.80E 00	0.2737E-01
0.10E 01	0.4117E-01
0.12E 01	0.5518E-01
0.14E 01	0.6751E-01
0.16E 01	0.7831E-01
0.18E 01	0.8774E-01
0.20E 01	0.9594E-01
0.22E 01	0.1030E 00
0.24E 01	0.1091E 00
0.26E 01	0.1143E 00
0.28E 01	0.1187E 00
0.30E 01	0.1224E 00
0.32E 01	0.1254E 00
0.34E 01	0.1279E 00
0.36E 01	0.1298E 00
0.38E 01	0.1313E 00
0.40E 01	0.1323E 00
0.42E 01	0.1330E 00
0.44E 01	0.1334E 00
0.46E 01	0.1335E 00
0.48E 01	0.1333E 00
0.50E 01	0.1328E 00
0.52E 01	0.1322E 00
0.54E 01	0.1314E 00
0.56E 01	0.1305E 00
0.58E 01	0.1294E 00
0.60E 01	0.1281E 00
0.62E 01	0.1268E 00
0.64E 01	0.1254E 00
0.66E 01	0.1239E 00
0.68E 01	0.1224E 00
0.70E 01	0.1208E 00
0.72E 01	0.1191E 00
0.74E 01	0.1174E 00
0.76E 01	0.1157E 00
0.78E 01	0.1140E 00
0.80E 01	0.1122E 00
0.82E 01	0.1104E 00
0.84E 01	0.1086E 00
0.86E 01	0.1069E 00
0.88E 01	0.1051E 00
0.90E 01	0.1033E 00
0.92E 01	0.1015E 00
0.94E 01	0.9976E-01
0.96E 01	0.9800E-01
0.98E 01	0.9626E-01
0.10E 02	0.9454E-01

T1 T2 ARE 0.100E 02 0.100E 00

TIME	OUTPUT
0.0	-0.2980E-06
0.20E 00	0.1127E 00
0.40E 00	0.2969E 00
0.60E 00	0.4875E 00
0.80E 00	0.6756E 00
0.10E 01	0.8602E 00
0.12E 01	0.9285E 00
0.14E 01	0.9217E 00
0.16E 01	0.9050E 00
0.18E 01	0.8873E 00
0.20E 01	0.8698E 00
0.22E 01	0.8525E 00
0.24E 01	0.8357E 00
0.26E 01	0.8191E 00
0.28E 01	0.8029E 00
0.30E 01	0.7870E 00
0.32E 01	0.7714E 00
0.34E 01	0.7561E 00
0.36E 01	0.7412E 00
0.38E 01	0.7265E 00
0.40E 01	0.7121E 00
0.42E 01	0.6980E 00
0.44E 01	0.6842E 00
0.46E 01	0.6706E 00
0.48E 01	0.6574E 00
0.50E 01	0.6443E 00
0.52E 01	0.6316E 00
0.54E 01	0.6191E 00
0.56E 01	0.6068E 00
0.58E 01	0.5948E 00
0.60E 01	0.5830E 00
0.62E 01	0.5715E 00
0.64E 01	0.5602E 00
0.66E 01	0.5491E 00
0.68E 01	0.5382E 00
0.70E 01	0.5275E 00
0.72E 01	0.5171E 00
0.74E 01	0.5069E 00
0.76E 01	0.4968E 00
0.78E 01	0.4870E 00
0.80E 01	0.4773E 00
0.82E 01	0.4679E 00
0.84E 01	0.4586E 00
0.86E 01	0.4495E 00
0.88E 01	0.4406E 00
0.90E 01	0.4319E 00
0.92E 01	0.4234E 00
0.94E 01	0.4150E 00
0.96E 01	0.4068E 00
0.98E 01	0.3987E 00
0.10E 02	0.3908E 00

T1 T2 ARE 0.100E 02 0.500E 00

TIME	OUTPUT
0.0	0.5960E-07
0.20E 00	0.3492E-01
0.40E 00	0.1229E 00
0.60E 00	0.2452E 00
0.80E 00	0.3892E 00
0.10E 01	0.5466E 00
0.12E 01	0.6768E 00
0.14E 01	0.7580E 00
0.16E 01	0.8063E 00
0.18E 01	0.8328E 00
0.20E 01	0.8448E 00
0.22E 01	0.8472E 00
0.24E 01	0.8432E 00
0.26E 01	0.8351E 00
0.28E 01	0.8243E 00
0.30E 01	0.8113E 00
0.32E 01	0.7983E 00
0.34E 01	0.7842E 00
0.36E 01	0.7699E 00
0.38E 01	0.7554E 00
0.40E 01	0.7410E 00
0.42E 01	0.7266E 00
0.44E 01	0.7125E 00
0.46E 01	0.6985E 00
0.48E 01	0.6849E 00
0.50E 01	0.6713E 00
0.52E 01	0.6581E 00
0.54E 01	0.6451E 00
0.56E 01	0.6323E 00
0.58E 01	0.6198E 00
0.60E 01	0.6075E 00
0.62E 01	0.5955E 00
0.64E 01	0.5837E 00
0.66E 01	0.5722E 00
0.68E 01	0.5609E 00
0.70E 01	0.5497E 00
0.72E 01	0.5389E 00
0.74E 01	0.5282E 00
0.76E 01	0.5177E 00
0.78E 01	0.5075E 00
0.80E 01	0.4974E 00
0.82E 01	0.4876E 00
0.84E 01	0.4779E 00
0.86E 01	0.4685E 00
0.88E 01	0.4592E 00
0.90E 01	0.4501E 00
0.92E 01	0.4412E 00
0.94E 01	0.4325E 00
0.96E 01	0.4239E 00
0.98E 01	0.4155E 00
0.10E 02	0.4073E 00

T1 T2 ARE 0.100E 02 0.100E 01

TIME	OUTPUT
0.0	0.0
0.20E 00	0.1960E-01
0.40E 00	0.6936E-01
0.60E 00	0.1457E 00
0.80E 00	0.2424E 00
0.10E 01	0.3550E 00
0.12E 01	0.4614E 00
0.14E 01	0.5451E 00
0.16E 01	0.6103E 00
0.18E 01	0.6605E 00
0.20E 01	0.6984E 00
0.22E 01	0.7263E 00
0.24E 01	0.7460E 00
0.26E 01	0.7592E 00
0.28E 01	0.7671E 00
0.30E 01	0.7706E 00
0.32E 01	0.7707E 00
0.34E 01	0.7680E 00
0.36E 01	0.7631E 00
0.38E 01	0.7564E 00
0.40E 01	0.7483E 00
0.42E 01	0.7392E 00
0.44E 01	0.7292E 00
0.46E 01	0.7185E 00
0.48E 01	0.7074E 00
0.50E 01	0.6959E 00
0.52E 01	0.6842E 00
0.54E 01	0.6724E 00
0.56E 01	0.6604E 00
0.58E 01	0.6485E 00
0.60E 01	0.6366E 00
0.62E 01	0.6248E 00
0.64E 01	0.6130E 00
0.66E 01	0.6014E 00
0.68E 01	0.5899E 00
0.70E 01	0.5786E 00
0.72E 01	0.5674E 00
0.74E 01	0.5564E 00
0.76E 01	0.5455E 00
0.78E 01	0.5349E 00
0.80E 01	0.5244E 00
0.82E 01	0.5142E 00
0.84E 01	0.5041E 00
0.86E 01	0.4941E 00
0.88E 01	0.4844E 00
0.90E 01	0.4749E 00
0.92E 01	0.4655E 00
0.94E 01	0.4563E 00
0.96E 01	0.4473E 00
0.98E 01	0.4385E 00
0.10E 02	0.4298E 00

T1 T2 ARE 0.100E 02 0.200E 01

TIME	OUTPUT
0.0	0.0
0.20E 00	0.9609E-02
0.40E 00	0.3696E-01
0.60E 00	0.7999E-01
0.80E 00	0.1368E 00
0.10E 01	0.2059E 00
0.12E 01	0.2759E 00
0.14E 01	0.3375E 00
0.16E 01	0.3915E 00
0.18E 01	0.4397E 00
0.20E 01	0.4797E 00
0.22E 01	0.5152E 00
0.24E 01	0.5457E 00
0.26E 01	0.5717E 00
0.28E 01	0.5937E 00
0.30E 01	0.6120E 00
0.32E 01	0.6272E 00
0.34E 01	0.6394E 00
0.36E 01	0.6491E 00
0.38E 01	0.6565E 00
0.40E 01	0.6617E 00
0.42E 01	0.6652E 00
0.44E 01	0.6670E 00
0.46E 01	0.6673E 00
0.48E 01	0.6664E 00
0.50E 01	0.6642E 00
0.52E 01	0.6611E 00
0.54E 01	0.6571E 00
0.56E 01	0.6523E 00
0.58E 01	0.6468E 00
0.60E 01	0.6407E 00
0.62E 01	0.6341E 00
0.64E 01	0.6271E 00
0.66E 01	0.6197E 00
0.68E 01	0.6119E 00
0.70E 01	0.6039E 00
0.72E 01	0.5956E 00
0.74E 01	0.5871E 00
0.76E 01	0.5785E 00
0.78E 01	0.5698E 00
0.80E 01	0.5610E 00
0.82E 01	0.5521E 00
0.84E 01	0.5432E 00
0.86E 01	0.5343E 00
0.88E 01	0.5254E 00
0.90E 01	0.5165E 00
0.92E 01	0.5076E 00
0.94E 01	0.4988E 00
0.96E 01	0.4900E 00
0.98E 01	0.4813E 00
0.10E 02	0.4727E 00

T1 T2 ARE 0.500E 00 0.200E 01

TIME	OUTPUT
0.0	0.0
0.20E 00	0.8495E-02
0.40E 00	0.2907E-01
0.60E 00	0.5632E-01
0.80E 00	0.8677E-01
0.10E 01	0.1182E 00
0.12E 01	0.1408E 00
0.14E 01	0.1500E 00
0.16E 01	0.1509E 00
0.18E 01	0.1467E 00
0.20E 01	0.1396E 00
0.22E 01	0.1309E 00
0.24E 01	0.1215E 00
0.26E 01	0.1120E 00
0.28E 01	0.1027E 00
0.30E 01	0.9386E-01
0.32E 01	0.8555E-01
0.34E 01	0.7782E-01
0.36E 01	0.7069E-01
0.38E 01	0.6415E-01
0.40E 01	0.5817E-01
0.42E 01	0.5272E-01
0.44E 01	0.4776E-01
0.46E 01	0.4325E-01
0.48E 01	0.3916E-01
0.50E 01	0.3545E-01
0.52E 01	0.3209E-01
0.54E 01	0.2904E-01
0.56E 01	0.2628E-01
0.58E 01	0.2379E-01
0.60E 01	0.2153E-01
0.62E 01	0.1948E-01
0.64E 01	0.1763E-01
0.66E 01	0.1595E-01
0.68E 01	0.1443E-01
0.70E 01	0.1306E-01
0.72E 01	0.1182E-01
0.74E 01	0.1069E-01
0.76E 01	0.9675E-02
0.78E 01	0.8754E-02
0.80E 01	0.7921E-02
0.82E 01	0.7167E-02
0.84E 01	0.6485E-02
0.86E 01	0.5868E-02
0.88E 01	0.5310E-02
0.90E 01	0.4804E-02
0.92E 01	0.4347E-02
0.94E 01	0.3934E-02
0.96E 01	0.3559E-02
0.98E 01	0.3221E-02
0.10E 02	0.2914E-02

T1 T2 ARE 0.5CCE C1 C.2CCE C1

TIME	CUTPUT
0.C	0.C
C.20E C0	C.9548E-C2
C.4CE CC	0.3647E-01
C.6CE CC	C.7839E-C1
C.8CE CC	C.1332E C0
C.10E 01	C.199CE CC
C.12E C1	0.2646E CC
C.14E C1	C.3206E 0C
C.16E C1	C.3681E CC
C.18E C1	C.4C81E CC
C.20E C1	C.4413E 0C
C.22E C1	0.4685E CC
C.24E C1	C.49C4E CC
C.26E C1	C.5C76E CC
C.28E 01	C.52C7E 0C
C.30E C1	0.5301E C0
C.32E C1	C.5363E C0
C.34E C1	0.5397E 00
C.36E C1	C.5406E C0
C.38E C1	0.5394E CC
C.40E C1	C.5364E 0C
C.42E C1	C.5317E CC
C.44E 01	C.5257E 00
C.46E C1	C.5185E CC
C.48E C1	C.51C3E 00
C.50E 01	C.5C12E 00
C.52E C1	0.4915E CC
C.54E C1	C.4812E 00
C.56E C1	C.47C5E CC
C.58E C1	C.4594E C0
C.6CE C1	0.4481E 00
C.62E C1	0.4365E CC
C.64E 01	C.4248E CC
C.66E 01	C.4131E 00
C.68E C1	C.4C14E 00
C.70E C1	0.3897E CC
C.72E 01	0.3781E C0
C.74E C1	C.3665E C0
C.76E C1	0.3552E CC
C.78E C1	C.3439E CC
C.80E C1	0.3329E 00
C.82E C1	0.3221E 00
C.84E C1	C.3114E C0
C.86E C1	C.3010E CC
C.88E C1	C.29C9E 00
C.90E C1	C.281CE 0C
0.92E 01	C.2713E 0C
C.94E C1	0.2619E C0
C.96E 01	C.2527E C0
C.98E C1	C.2438E 00
C.10E 02	0.2351E 00

T1 T2 ARE 0.400E 00 0.500E 00

TIME	OUTPUT
0.0	-0.9537E-06
0.20E 00	0.2981E-01
0.40E 00	0.8995E-01
0.60E 00	0.1546E 00
0.80E 00	0.2127E 00
0.10E 01	0.2607E 00
0.12E 01	0.2684E 00
0.14E 01	0.2367E 00
0.16E 01	0.1932E 00
0.18E 01	0.1504E 00
0.20E 01	0.1135E 00
0.22E 01	0.8376E-01
0.24E 01	0.6081E-01
0.26E 01	0.4359E-01
0.28E 01	0.3094E-01
0.30E 01	0.2178E-01
0.32E 01	0.1523E-01
0.34E 01	0.1059E-01
0.36E 01	0.7332E-02
0.38E 01	0.5056E-02
0.40E 01	0.3474E-02
0.42E 01	0.2381E-02
0.44E 01	0.1627E-02
0.46E 01	0.1110E-02
0.48E 01	0.7555E-03
0.50E 01	0.5135E-03
0.52E 01	0.3484E-03
0.54E 01	0.2361E-03
0.56E 01	0.1599E-03
0.58E 01	0.1081E-03
0.60E 01	0.7304E-04
0.62E 01	0.4931E-04
0.64E 01	0.3326E-04
0.66E 01	0.2243E-04
0.68E 01	0.1511E-04
0.70E 01	0.1018E-04
0.72E 01	0.6850E-05
0.74E 01	0.4609E-05
0.76E 01	0.3100E-05
0.78E 01	0.2084E-05
0.80E 01	0.1401E-05
0.82E 01	0.9416E-06
0.84E 01	0.6326E-06
0.86E 01	0.4249E-06
0.88E 01	0.2853E-06
0.90E 01	0.1916E-06
0.92E 01	0.1286E-06
0.94E 01	0.8623E-07
0.96E 01	0.5794E-07
0.98E 01	0.3888E-07
0.10E 02	0.2609E-07

T1 T2 ARE 0.200E 01 0.500E 00

TIME	OUTPUT
0.0	0.5960E-06
0.20E 00	0.3398E-01
0.40E 00	0.1163E 00
0.60E 00	0.2253E 00
0.80E 00	0.3471E 00
0.10E 01	0.4728E 00
0.12E 01	0.5630E 00
0.14E 01	0.6000E 00
0.16E 01	0.6037E 00
0.18E 01	0.5870E 00
0.20E 01	0.5584E 00
0.22E 01	0.5235E 00
0.24E 01	0.4860E 00
0.26E 01	0.4480E 00
0.28E 01	0.4108E 00
0.30E 01	0.3754E 00
0.32E 01	0.3422E 00
0.34E 01	0.3113E 00
0.36E 01	0.2828E 00
0.38E 01	0.2566E 00
0.40E 01	0.2327E 00
0.42E 01	0.2109E 00
0.44E 01	0.1910E 00
0.46E 01	0.1730E 00
0.48E 01	0.1566E 00
0.50E 01	0.1418E 00
0.52E 01	0.1284E 00
0.54E 01	0.1162E 00
0.56E 01	0.1051E 00
0.58E 01	0.9515E-01
0.60E 01	0.8610E-01
0.62E 01	0.7791E-01
0.64E 01	0.7050E-01
0.66E 01	0.6380E-01
0.68E 01	0.5773E-01
0.70E 01	0.5224E-01
0.72E 01	0.4727E-01
0.74E 01	0.4277E-01
0.76E 01	0.3870E-01
0.78E 01	0.3502E-01
0.80E 01	0.3168E-01
0.82E 01	0.2867E-01
0.84E 01	0.2594E-01
0.86E 01	0.2347E-01
0.88E 01	0.2124E-01
0.90E 01	0.1922E-01
0.92E 01	0.1739E-01
0.94E 01	0.1573E-01
0.96E 01	0.1424E-01
0.98E 01	0.1288E-01
0.10E 02	0.1166E-01